

# Photoacoustic observation of the HOWMANYnm absorption line in O<sub>2</sub>

Zeno Tornasi, Michele Valentini, Henry Widodo

August 24, 2013

# Contents

<b>Introduction</b>	<b>3</b>
<b>1 Experimental apparatus</b>	<b>4</b>
1.1 The laser source . . . . .	4
1.2 The acoustic chamber . . . . .	5
<b>A Extended Cavity Diode Laser</b>	<b>6</b>
<b>B The etalon</b>	<b>9</b>
B.1 Introduction . . . . .	9
B.2 Theoretical treatment . . . . .	9
B.3 Interference pattern . . . . .	13
B.4 Etalon as a spectroscope . . . . .	14

## **Introduction**

In this report we will write about the experiment done during the first and second weeks of August in order to measure one "line" in the visible part of the absorption spectrum (ATMOSPHERIC BAND/B-BAND?) of the Oxygen molecule using the photoacoustic effect. In order to excite the oxygen molecular orbitals we used a diode laser tuned with an external cavity. INSERT SMALL RESUME OF THE REPORT? FOR EXAMPLE (IN CHAPTER 1 WE WILL TALK ABOUT BLABLA, IN CHAMPTER 2 ABOUT BLIBLI ETC?)

# 1 Experimental apparatus

The setup we used featured the typical photoacoustic experiment characteristics. There was a source of light, a laser in our case, impinging on the gas into a cavity. A mechanical chopper provided a modulation of the light in order to match a proper frequency of the cavity. The acoustic signal, detected by microphones, was filtered by a lock-in amplifier referenced with the chopping frequency. The light path was controlled through optical elements such as mirrors, lenses and beam-splitters. Some standard laboratory instrumentation was used as well, including:

- generator
- waveform generator
- oscilloscope
- optical fiber spectroscope
- membrane vacuum pump
- etalon
- analogic videocamera
- monitor

We'll now describe in more details the main elements of the apparatus.

## 1.1 The laser source

We used an external cavity laser device, formed by the following elements:

- a single mode multi-quantum well AlGaInP laser diode<sup>1</sup>. The lasing wavelength could be tuned from about 680 nm to 695 nm by adjusting the driving current and the diode temperature.
- a temperature controller case<sup>2</sup> to set the temperature of the diode.
- an external cavity, i.e. a setup that feeds back the laser diode with the first diffraction order of a 1800 grooves/mm grating. The external cavity allowed us to better select a given lasing mode, thus getting a smaller emission linewidth. The grating was put on a piezoelectric mechanical actuator, which permitted nm-order adjustments of its position. Since a grating diffracts different frequencies at different angles, moving the grating we could control the frequency fed back to the laser and thus enhanced. This is how we got a fine tuning of the frequency, and how we were able to make the HOWMANYGHz scan to see the absorption line.

---

<sup>1</sup>Hitachi HL6738MG: [http://pdf.datasheetcatalog.com/datasheets/50/502031\\_DS.pdf](http://pdf.datasheetcatalog.com/datasheets/50/502031_DS.pdf)

<sup>2</sup>Thorlabs TCLDM9: <http://www.thorlabs.de/Thorcat/1900/TCLDM9-Manual.pdf>

## 1.2 The acoustic chamber

The gas to analyze, pure O<sub>2</sub> at atmospheric pressure, was contained in a brass chamber, featuring :

- an internal cavity, about 13 cm long, where the gas actually resonated. Other two smaller cavities were present before and after the main cavity. Since we couldn't open the brass chamber, we had no way to accurately measure the dimensions and the position of the main cavity with respect to the other two ones. It should be noticed that our chamber had been recycled from another experiment and was not explicitly thought for the usage we do of it. However, there were two marks on the outer side of the chamber, that were supposed to indicate where the main cavity started and ended.
- four microphones put about halfway in the chamber, one for each side of it. Due to the fact that the chamber couldn't be opened, we don't know whether the microphones were actually halfway. According to the marks, they were not. In fact, they were 5 mm away from the supposed middle point.
- an active strain gauge vacuometer<sup>3</sup> measured the pressure in the chamber.

---

<sup>3</sup>Edwards ASG-1000-NW16:

<http://www.ultimatevacuum.dk/D35725880%20ASG%20user%20manual.pdf>

## A Extended Cavity Diode Laser

The light emitted by a diode laser greatly diverges in an oval shape pattern. Such a wide beam is practically useless to an experimentalist. Therefore, it is necessary to collimate the output of the diode laser, that is, bend the diverging light through a lens (or several lenses) so that all the output goes in one direction. One can achieve this result using a single lens as long as the laser is placed exactly at the focal point of the lens one chooses. The focal point of a lens is also the point through which all light parallel to its normal axis will converge. Hence, if we place our diode laser at the focal point of our collimating lens all light from the diode laser that passes through the lens will exit parallel to the normal axis and all light that enters the face of the lens at normal incidence will be focused by the diode laser. This property of optics allows us to send optical feedback back into the laser. Because of its small cavity, diode lasers have a large bandwidth, which means that the laser emits light over a broader range of wavelengths than other lasers.

The broad linewidth of solitary diode laser often reduces their usefulness for spectroscopy applications. To overcome this problem several techniques have been developed, for example:

1. negative electronic feedback
2. resonant optical feedback from a high-finesse optical cavity
3. extended-cavity configurations

Among all these techniques that can be used to reduce the laser linewidth down to the kHz range, the extended-cavity configuration with grating feedback has become the most popular. It provides a simple means to achieve a wide wavelength tuning range and a narrow linewidth. Several reasons, why we need to construct good external cavity:

1. an external cavity is capable of producing very short, sharp pulse in the range of picoseconds by means of mode-locking.
2. the external cavity provides high modal stability through optical feedback; mode hoping is severely reduced.
3. a very narrow linewidth can be obtained by coupling a laser diode to an external cavity.

There are 3 cavities which set up in experiments:

1. Laser diode cavity or Fabry-Perot cavity
2. External cavity between grating and back side of the diode
3. Parasitic cavity between grating and the front facet of the diode

One of the ways to narrow the bandwidth of a diode laser is to use optical feedback to drive the laser at a single allowed lasing frequency. The collimation lens of the ECDL (Extended Cavity Diode Laser) is one critical part of attaining optical feedback. The second part of our system that allows optical feedback is the diffraction grating. A diffraction grating is finely scored reflective material that, due to its geometry, allows

only certain wavelengths of light incident at an angle to interfere constructively with itself as it is reflected outward. The formula for constructively diffracted orders of light reflected from a diffraction grating is:

$$d \sin \theta = m\lambda \quad (1)$$

where  $d$  is the spacing between reflective surfaces,  $\theta$  is the angle of incidence,  $\lambda$  is the wavelength of the incident light and  $m$  is an integer. One consequence of the above equation is that spectra diffracted off a grating are reproduced at several different angular positions about the grating. The various replications of the spectra are called *orders of diffraction* and obey the following relationship

$$\sin \theta_i + \sin \theta_m = Nm \quad (2)$$

where  $\theta_m$  is the angle of the  $m$ th order diffracted beam,  $N$  is the spatial frequency of the grating (units  $\text{nm}^{-1}$ ), and  $\theta_i$ ,  $m$ , are incident angle, integer, and wavelength.

A schematic layout of the extended-cavity laser is outlined in grating. The laser system consists of a diode laser as the active medium, a collimating lens and a diffraction grating. The external cavity is formed between the rear facet of the diode laser and the grating as a wavelength selective mirror. The laser frequency depends critically on the optical length of the cavity, which is sensitive to any changes in the refractive index of the cavity medium (diode laser, lens, and air) and to changes in the physical cavity length.

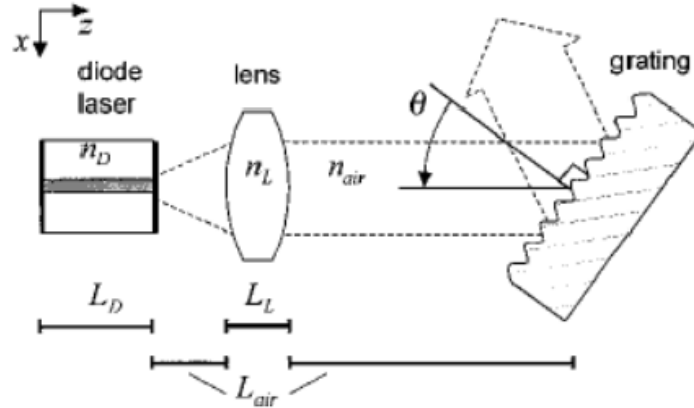


**Figure 1:** Schematic layout of the extended cavity laser. The total optical path length in the cavity is  $L_{EC} = L_D n_D + L_L n_L + L_{air} n_{air}$

The frequency of a solitary diode laser is sensitive to variations in the injection current and the junction temperature. This is mainly caused by changes in the refractive index of the active medium. The optical length of the collimating lens changes with temperature. This is caused by thermal expansion of the material and temperature dependence of the refractive index. Their effects on the laser frequency can be written as

$$\frac{d\nu}{dT_L} = -\nu \frac{L_L}{L_{EC}} (\alpha_L (n_L - n_{air} + \beta_L n_L)) \quad (3)$$

where  $n_L$  and  $n_{air}$  are the refractive indices of the lens material and air, and  $L_L$  and  $L_{EC}$  are the physical length of the lens and the total optical path length of the external cavity, respectively. The thermal expansion coefficient of the lens material is denoted by  $\alpha_L$  and the relative temperature coefficient of the refractive index by  $\beta_L$ .

The refractive index of air is mainly sensitive to variations in pressure  $p$  and temperature  $T_{air}$ . Their effects on the laser frequency can be written as

$$\frac{d\nu}{dp} = -\nu \frac{L_{air}}{L_{EC}} \frac{dn_{air}}{dp} \quad (4)$$

and

$$\frac{d\nu}{dT_{air}} = -\nu \frac{L_{air}}{L_{EC}} \frac{dn_{air}}{dT_{air}} \quad (5)$$

where  $L_{air}$  is the cavity length containing air.

The mechanical structure of the cavity often contains micrometer screws and piezoelectric transducers (PZTs) for wavelength control. The sensitivity of the laser frequency to thermal expansion of these parts can be written as

$$\frac{d\nu}{dT_m} = \pm\nu \frac{L_m \alpha_m}{L_{EC}} \quad (6)$$

where  $L_m$  and  $\alpha_m$  are the length and the thermal expansion coefficient of the mechanical part, respectively.

A transverse displacement along  $x$  axis of the collimating lens with respect to the laser diode changes the beam direction. This causes a frequency shift due to a change in the cavity length. For a small displacement, the frequency shift can be written as

$$\frac{d\nu}{dx} = \frac{\nu \tan \theta}{f_L} \quad (7)$$

$$\frac{d\nu_G}{dT} = -\nu_G \alpha_G \quad (8)$$

where  $f_L$  is the focal length of the lens and  $\theta$  is the angle between the grating normal and the incident beam, while  $\nu_G$  and  $\alpha_G$  are the center frequency of the grating feedback and the grating thermal expansion coefficient respectively. The displacement of the lens can be caused, for example, by asymmetric thermal expansion relative to the optical axis or by mechanical vibration of the lens holder.

There are additional effects that influence mainly the short-term frequency stability of the laser: current- and PZT driver noise, mechanical vibrations, acoustic disturbances, and rapid changes in the refractive index of air caused by air flow. All of these factors have an effect on the length of the external cavity and, consequently, generate frequency modulation of the laser.

## B The etalon

### B.1 Introduction

The etalon is an optical device made of two perfectly parallel semi-reflecting surfaces. It can be thought as a Fabry-Pérot cavity which walls are fixed. This geometry can be implemented either with an air-based or a solid design. The first one consist in two surfaces separated by air, one of which usually can be moved via piezoelectric actuators. The second one is just made from a piece of glass (or other materials suitable for the desired application) with a partially reflecting coating covered facets (Fig. 2). While the air based etalons make longer cavities, thus more precise, they are extremely delicate and cumbersome to manage, mostly because the two surfaces must be kept parallel within hundredths of wavelength. The solid state ones, on the other hand, are usually smaller and less performing, but way more robust and easier to use.

Every time the impinging beam encounters one of the two optical surfaces the light is partially reflected and partially transmitted. Multiple reflections occur inside the two surfaces leading to an infinite number of rays departing from the interferometer in both the transmitted and reflected directions. Contiguous beams differ for a constant phase and this causes an interference pattern, as shown in Fig. 3.

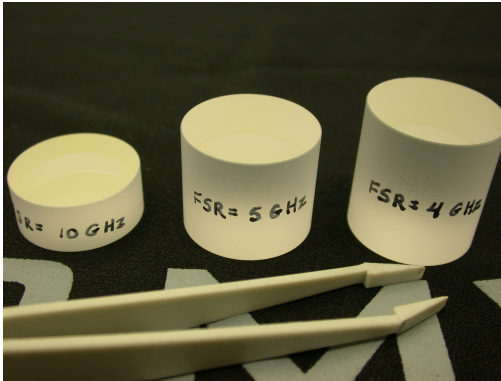


**Figure 2:** Solid state etalons.



**Figure 3:** The etalon diffraction pattern seen through our videocamera.

### B.2 Theoretical treatment

To derive the phase difference between two adjacent beams, let's begin calculating the difference in their optical paths (Fig. 4). We thus choose two parallel beams, such as  $OB$  and  $CD$ , and draw a wavefront perpendicular to them,  $AC$ . The optical path difference between  $A$  and  $C$  is given by

$$\overline{ABC} = \overline{AB} + \overline{BC} \quad (9)$$

We call  $d$  the width of the etalon, and  $s$  the distance traveled by the beam from one surface to the other one, so that

$$\overline{BC} = \overline{OB} \equiv s = \frac{d}{\cos \theta'}. \quad (10)$$

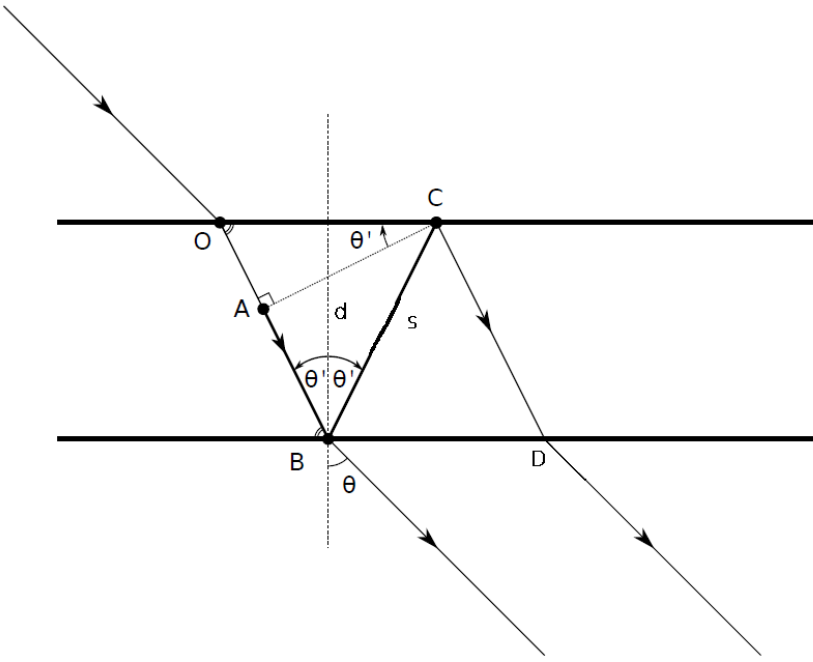


**Figure 4:** The impinging beam changes direction due to refraction index difference between the air and the glass, the angles  $\theta$  and  $\theta'$  being related to the refraction indices  $n$  and  $n'$  by Snell's law.

From elementary geometry considerations we get the following relationships:

$$\overline{AB} = \overline{OB} - \overline{OA} \quad (11)$$

$$\overline{OA} = \sqrt{\overline{OC}^2 - \overline{AC}^2} \quad (12)$$

$$\overline{OC} = 2s \sin \theta' \quad (13)$$

$$\overline{AC} = s \sin(2\theta') \quad (14)$$

Then we write

$$\begin{aligned} \overline{OA} &= \sqrt{4s^2 \sin^2 \theta' - s^2 \sin^2(2\theta')} \\ &= \sqrt{4s^2 \sin^2 \theta' \left(1 - \frac{\sin^2(2\theta')}{4 \sin^2 \theta'}\right)} \\ &= 2s \sin \theta' \sqrt{1 - \cos^2 \theta'} \\ &= 2s \sin^2 \theta' \end{aligned} \quad (15)$$

Putting all together we get the optical path difference

$$\begin{aligned} \overline{ABC} &= \overline{AB} + \overline{BC} \\ &= \overline{OB} - \overline{OA} + \overline{BC} \\ &= s - 2s \sin^2 \theta' + s \\ &= 2s(1 - \sin^2 \theta') \\ &= 2s \cos^2 \theta' \\ &= 2d \cos \theta'. \end{aligned} \quad (16)$$

If the incident light has wavelength  $\lambda_0$  in the vacuum and the etalon medium has refractive index  $n'$ , the light wave vector inside the medium is

$$k = \frac{2\pi}{\lambda_0} n' \quad (17)$$

and the phase shift between two adjacent rays is

$$\Delta = k \cdot \overline{ABC} = \frac{4\pi}{\lambda_0} n' d \cos \theta' \quad (18)$$

Now, indicating by  $T$  the overall etalon transmission coefficient and by  $R$  the reflection coefficient corresponding to one round-trip, the total amplitude of the electric field in some point after the etalon is the sum of those of the subsequent rays

$$E_T = E_0 T + E_0 T R e^{i\Delta} + E_0 T R^2 e^{i2\Delta} + E_0 T R^3 e^{i3\Delta} + \dots \quad (19)$$

which is nothing but the geometrical series, that can be summed up ( $|Re^{i\Delta}| < 1$ ) to yield

$$E_T = E_0 T \sum_j (R e^{i\Delta})^j = \frac{E_0 T}{1 - R e^{i\Delta}} \quad (20)$$

What we observe is actually the transmitted intensity

$$I_T = |E_T|^2 = |E_0|^2 \frac{T^2}{|1 - R e^{i\Delta}|^2} \quad (21)$$

The denominator can be rewritten as

$$\begin{aligned} |1 - R e^{i\Delta}| &= (1 - R e^{i\Delta})(1 - R e^{-i\Delta}) \\ &= 1 - R(e^{i\Delta} + e^{-i\Delta}) + R^2 \\ &= 1 - 2R \cos \Delta + R^2 \\ &= 1 - 2R \left(1 - 2 \sin^2 \frac{\Delta}{2}\right) + R^2 \\ &= 1 - 2R + 4R \sin^2 \frac{\Delta}{2} + R^2 \\ &= (1 - R)^2 + 4R \sin^2 \frac{\Delta}{2} \\ &= (1 - R)^2 \left(1 + \frac{4R}{(1 - R)^2} \sin^2 \frac{\Delta}{2}\right) \end{aligned} \quad (22)$$

So that the transmitted intensity becomes

$$I_T = I_0 \frac{T^2}{(1 - R)^2} \frac{1}{\left(1 + \frac{4R}{(1 - R)^2} \sin^2 \frac{\Delta}{2}\right)} \quad (23)$$

One defines a *peak constant*

$$C_{\text{peak}} \equiv \frac{T^2}{(1 - R)^2} \quad (24)$$

which is equal to 1 for an ideal surface such that  $1 = R + T$ . In a real surface, instead, some absorption  $A$  is present, so that  $1 = R + T + A$ . The peak constant in this case can be rewritten as

$$C_{\text{peak}} = \frac{(1 - A - R)^2}{(1 - R)^2} = \left(1 - \frac{A}{1 - R}\right)^2 \quad (25)$$

Furthermore we shall define the *coefficient of finesse*<sup>4</sup>

$$F \equiv \frac{4R}{(1 - R)^2}. \quad (26)$$

In the ideal etalon case we have  $A \simeq 0$ , which implies  $C_{\text{peak}} \simeq 1$ , so that Eq. (23) eventually reduces to

$$I_T = I_0 \frac{1}{1 + F \sin^2 \frac{\Delta}{2}} \quad (27)$$

The transmitted intensity is thus given by the constant input intensity value, modulated by the so called *Airy function* plotted in Fig. 5

$$\frac{I_T}{I_0} = \frac{1}{1 + F \sin^2 \frac{\Delta}{2}} \equiv A[F; \Delta] \quad (28)$$

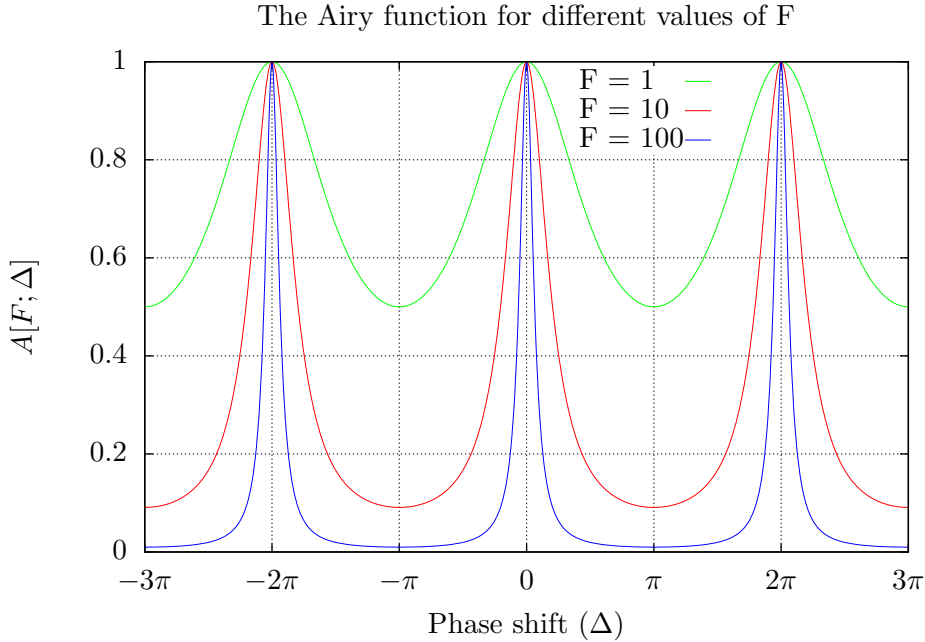


**Figure 5:** The Airy function peaks when the phase shift is an integer multiple of  $2\pi$ . As the finesse coefficient increases, the peaks become more sharp and their position is better defined.

---

<sup>4</sup>Not to be confused with the *finesse* defined further in this discussion at pg. 13. These two parameters are strongly correlated, though, and literature is not uniform on which of the two is to be called "finesse".

### B.3 Interference pattern

As is clear from Fig. 5, the interference maxima take place for  $\Delta = 2m\pi$ , where  $m$  is an integer representing the order of diffraction. From Eq. (18) we have

$$m = \frac{2n'}{\lambda_0} d \cos \theta' \quad (29)$$

Looking at Eq. (23) we define the intensity at the maximum and at the minimum as

$$I_{\max} = \frac{I_T[\Delta = 2m\pi]}{I_0} = C_{\text{peak}} = \frac{T^2}{(1-R)^2} \quad (30)$$

$$I_{\min} = \frac{I_T[\Delta = (2m+1)\pi]}{I_0} = \frac{T^2}{(1-R)^2 + 4R} = \frac{T^2}{(1+R)^2} \quad (31)$$

We shall now define a *contrast factor*

$$\mathcal{C} \equiv \frac{I_{\max}}{I_{\min}} = \left( \frac{1+R}{1-R} \right)^2 = 1+F \quad (32)$$

which is also a useful parameter in the characterization of an etalon.

To describe how defined are the peaks, we have to consider their full width at half maximum (FWHM). Thus we observe the points around a maximum whose intensity is  $I_T = I_{\max}/2$ . They have a phase shift

$$\Delta = 2m\pi \pm \frac{\varepsilon}{2} \quad (33)$$

where  $\varepsilon$  is now the FWHM expressed as a phase. Putting this into Eq. (23) we get the identity

$$\begin{aligned} \frac{1}{2} &= \frac{1}{1+F \sin^2 \frac{\varepsilon}{4}} \quad ; \\ F \sin^2 \frac{\varepsilon}{4} &= 1 \end{aligned}$$

If now we approximate  $\sin \frac{\varepsilon}{4} \simeq \frac{\varepsilon}{4}$  we get the phase expression for the FWHM, as a function of the coefficient of finesse  $F$

$$\varepsilon = \frac{4}{\sqrt{F}} \quad (34)$$

Since two contiguous maxima are separated by a phase of  $2\pi$ , we can do the ratio between the peaks separation and their width, getting a very important parameter which is called the *finesse* of the etalon

$$\mathcal{F} \equiv \frac{2\pi}{\varepsilon} = \frac{\pi}{2} \sqrt{F} = \frac{\pi \sqrt{R}}{1-R} \quad (35)$$

## B.4 Etalon as a spectroscope

It is possible to build a direct relationship between the angular separation of the rings and the wavelength  $\lambda_0$  of the incident light. We put ourself under the approximation of nearly perpendicular incident light, so that

$$\sin \theta' \simeq \theta'$$

$$\sin \theta \simeq \theta$$

Snell's law then simplifies to

$$\frac{\sin \theta'}{n'} = \frac{\sin \theta}{n} \Rightarrow \frac{\theta'}{n'} = \frac{\theta}{n}$$

The small angles approximation also implies

$$\begin{aligned} \cos \theta' &\simeq 1 - \frac{\theta'^2}{2} \\ &\simeq 1 - \left(\frac{n'}{n}\right)^2 \frac{\theta^2}{2} \end{aligned}$$

These approximations being valid, we recall Eq. (29)

$$m = \frac{2n'}{\lambda_0} d \cos \theta' \Rightarrow m = \frac{2n'}{\lambda_0} d \left(1 - \left(\frac{n'}{n}\right)^2 \frac{\theta^2}{2}\right)$$

Inverting this one we find NON SI CAPISCHE DA DOVE LA TIRA FUORI E COME, CI SONO CONTI OSCURI [...] The angle for the  $p$ th order is

$$\theta_p = \frac{1}{n} \sqrt{\frac{n' \lambda_0}{d}} \sqrt{p - 1 + e} \quad (36)$$

and if we focus the rings onto a screen with a convergent lens, of focal ratio  $f$ , the diameter of the bright ring is

$$D_p^2 = (2f\theta_p)^2 = \frac{4n' \lambda_0 f^2}{n^2 d} (p - 1 + e) \quad (37)$$